

Are your **MRI contrast agents** cost-effective?

Learn more about generic **Gadolinium-Based Contrast Agents**.



**FRESENIUS  
KABI**

caring for life

# AJNR

## **Relationship between Shear Stiffness Measured by MR Elastography and Perfusion Metrics Measured by Perfusion CT of Meningiomas**

T. Takamura, U. Motosugi, M. Ogiwara, Y. Sasaki, K.J. Glaser, R.L. Ehman, H. Kinouchi and H. Onishi

This information is current as of June 4, 2024.

*AJNR Am J Neuroradiol* 2021, 42 (7) 1216-1222

doi: <https://doi.org/10.3174/ajnr.A7117>

<http://www.ajnr.org/content/42/7/1216>

# Relationship between Shear Stiffness Measured by MR Elastography and Perfusion Metrics Measured by Perfusion CT of Meningiomas

 T. Takamura,  U. Motosugi,  M. Ogiwara,  Y. Sasaki,  K.J. Glaser,  R.L. Ehman,  H. Kinouchi, and  H. Onishi



## ABSTRACT

**BACKGROUND AND PURPOSE:** When managing meningiomas, intraoperative tumor consistency and histologic subtype are indispensable factors influencing operative strategy. The purposes of this study were the following: 1) to investigate the correlation between stiffness assessed with MR elastography and perfusion metrics from perfusion CT, 2) to evaluate whether MR elastography and perfusion CT could predict intraoperative tumor consistency, and 3) to explore the predictive value of stiffness and perfusion metrics in distinguishing among histologic subtypes of meningioma.

**MATERIALS AND METHODS:** Mean tumor stiffness and relative perfusion metrics (blood flow, blood volume, and MTT) were calculated (relative to normal brain tissue) for 14 patients with meningiomas who underwent MR elastography and perfusion CT before surgery (cohort 1). Intraoperative tumor consistency was graded by a neurosurgeon in 18 patients (cohort 2, comprising the 14 patients from cohort 1 plus 4 additional patients). The correlation between tumor stiffness and perfusion metrics was evaluated in cohort 1, as was the ability of perfusion metrics to predict intraoperative tumor consistency and discriminate histologic subtypes. Cohort 2 was analyzed for the ability of stiffness to determine intraoperative tumor consistency and histologic subtypes.

**RESULTS:** The relative MTT was inversely correlated with stiffness ( $P = .006$ ). Tumor stiffness was positively correlated with intraoperative tumor consistency ( $P = .01$ ), while perfusion metrics were not. Relative MTT significantly discriminated transitional meningioma from meningothelial meningioma ( $P = .04$ ), while stiffness did not significantly differentiate any histologic subtypes.

**CONCLUSIONS:** In meningioma, tumor stiffness may be useful to predict intraoperative tumor consistency, while relative MTT may potentially correlate with tumor stiffness and differentiate transitional meningioma from meningothelial meningioma.

**ABBREVIATIONS:** BF = blood flow; BV = blood volume; CUSA = Clarity Ultrasonic Surgical Aspirator System; MRE = MR elastography; PCT = perfusion CT; rBF = relative BF; rBV = relative BV; rMTT = relative MTT

Meningioma is the most common primary intracranial tumor with an incidence of approximately 8 cases per 10,000 persons per year.<sup>1</sup> Radiosurgery, chemotherapy, or arterial embolization play supplementary roles, though surgical resection is the primary treatment for meningiomas. Tumor consistency is recognized as a major

indicator of complete resection for meningiomas.<sup>2</sup> To date, various imaging modalities including T2-weighted images, diffusion MR imaging measurements, and magnetization transfer imaging have been investigated to predict meningioma consistency.<sup>3</sup> However, there have been conflicting results, and no widely accepted method has been established.

MR elastography (MRE) is a dynamic MR imaging-based technique used for the noninvasive measurement of the mechanical properties of soft tissue *in vivo*.<sup>4</sup> Recently, the mechanical properties of the brain have been studied in normal aging,<sup>5-9</sup> Alzheimer disease,<sup>6,10,11</sup> Parkinson disease,<sup>12</sup> frontotemporal dementia,<sup>6</sup> normal pressure hydrocephalus,<sup>6</sup> and brain tumors,<sup>13</sup> including meningiomas.<sup>14-17</sup> More recently, slip interface imaging using specialized processing of MRE data was shown to provide a dynamic measure of adherence between the tumor and the adjacent brain tissue.<sup>18</sup>

The global shear modulus of soft biologic tissue can be influenced by the scale of perfusion,<sup>19</sup> which relates to the topology

Received June 20, 2020; accepted after revision January 10, 2021.

From the Department of Radiology (T.T.), Shizuoka General Hospital, Shizuoka, Japan; Department of Radiology (T.T.), Juntendo University, Tokyo, Japan; Department of Radiology (U.M.), Kofu-Kyoritsu Hospital, Yamanashi, Japan; Departments of Neurosurgery (M.O., H.K.) and Radiology (Y.S., H.O.), University of Yamanashi, Yamanashi, Japan; and Department of Radiology (K.J.G., R.L.E.), Mayo Clinic College of Medicine, Rochester, Minnesota.

This work was supported, in part, by the National Institutes of Health, R37 EB001981.

Please address correspondence to Tomohiro Takamura, MD, PhD, Department of Radiology, Shizuoka General Hospital, 4-27-1 Kita Ando Aoi-ku, Shizuoka City 420-8527, Japan; e-mail: t-takamura@i.shizuoka-pho.jp

 Indicates open access to non-subscribers at [www.ajnr.org](http://www.ajnr.org)

 Indicates article with online supplemental data.

<http://dx.doi.org/10.3174/ajnr.A717>

and geometry of microvessels,<sup>20</sup> indicating a potential effect of perfusion on the macroscopic viscoelastic response of brain tissue. Previous MRE studies have indicated a close correlation between tissue perfusion and mechanical properties in the brain<sup>21,22</sup> and abdominal organs.<sup>23</sup> Moreover, in investigations of the pathologic determinants underpinning MRE data,<sup>24,25</sup> microvascular density, which is related to perfusion metrics,<sup>21</sup> has been shown to contribute to the stiffness of soft brain tumor models in mice. Nevertheless, the perfusion conditions and mechanical properties of meningiomas have not been concurrently analyzed. Meningioma consistency and histologic subtype are indispensable factors influencing operative strategy and patient counseling. Recently, MRE has been increasingly recognized as a useful indicator of meningioma consistency,<sup>14-17</sup> while perfusion metrics provide physiologic and functional information about the tumor microenvironment. Because stiffness and perfusion status are intricately related, MRE and perfusion metrics may serve to preoperatively characterize the viscoelastic properties of meningiomas and further develop clinically applicable predictors for intraoperative tumor consistency. Relatively few studies have reported the relationship between stiffness<sup>16</sup> or perfusion metrics<sup>26-28</sup> and histologic subtype, and no definite association has been established. Investigating the relationship of stiffness and perfusion metrics to intraoperative meningioma consistency and histologic subtypes may contribute to understanding and objective comparison of these techniques and provide valuable information affecting risk assessment, patient management, and workflow optimization.

The purposes of this study were the following: 1) to investigate the correlation between stiffness and perfusion metrics, 2) to evaluate whether preoperative MRE and perfusion metrics could predict intraoperative tumor consistency, and 3) to explore the predictive value of stiffness and perfusion metrics in distinguishing among histologic subtypes of meningiomas.

## MATERIALS AND METHODS

### Subjects

This retrospective study was approved by institutional review board of University of Yamanashi Hospital. Between May 2017 and September 2019, twenty-seven meningiomas of 27 patients who underwent MRE and received pathologic confirmation of meningioma with subsequent radical resection were included in this study. For the correlation analysis between stiffness measured by MRE and perfusion metrics measured by perfusion CT (PCT), between perfusion metrics and intraoperative tumor consistency, as well as group analysis of pathologic subtype for perfusion metrics, patients were excluded under the following circumstances: 1) Preoperative endovascular embolization for tumors was performed, 2) tumors were clinically confirmed as locally recurring, 3) tumors were resected en bloc without the use of air aspiration or the Clarity Ultrasonic Surgical Aspirator System (CUSA; Integra LifeSciences), 4) there was no available PCT examination within 12 weeks of the MRE examination, or 5) PCT data were not successfully analyzed by the Perfusion Mismatch Analyzer software (PMA; ASIST Group). Of the 27 patients, we excluded 13 patients: Seven underwent endovascular embolization, 1 was a local recurrence case, 3 lacked an available PCT examination, and

2 were excluded because their PCT data were not successfully analyzed by the PMA software. Additionally, 1 of the 3 patients lacking an available PCT examination had undergone en bloc resection. The reason for the PCT data miscalculation by the PMA software in 1 case was the irregular arterial attenuation curve due to the presence of metal-related artifacts from previously implanted clips for a cerebral aneurysm independent of the meningioma. The reason for the other case was unclear.

Of these 13 excluded patients, 4 patients (2 lacked an available PCT and 2 whose PCT data were not successfully analyzed) who did not fulfill the following exclusion criteria (ie, 1) preoperative endovascular embolization for tumors was performed, 2) the tumors were clinically confirmed as locally recurring and, 3) the tumors were resected en bloc without the use of air aspiration or the CUSA) were additionally included in the correlation analysis between stiffness and intraoperative tumor consistency as well as the group analysis of pathologic subtype for stiffness because they were considered to have no intervention during the period between the MRE examination and the operation. Finally, 14 patients were included for the correlation analysis between stiffness and perfusion metrics, between perfusion metrics and intraoperative tumor consistency, and the group analysis of pathologic subtype for perfusion metrics (cohort 1), while 18 patients were included for the correlation analysis between stiffness and intraoperative tumor consistency and the group analysis of pathologic subtype for stiffness (cohort 2).

### Surgical Assessment of Tumor Consistency

Intraoperative tumor consistency was defined on the basis of the CUSA amplitude applied for tumor removal. The CUSA amplitude setting was determined in 10 steps and ranged from 10% to 100%. These values were consistently chosen by 1 operating neurosurgeon (M.O.) for all cases. The intraoperative tumor consistency score was defined as a value of 1/10 of the CUSA amplitude (eg, a CUSA amplitude of 50% was defined as score 5). If the tumor was removed solely by using air aspiration without the use of CUSA, the intraoperative tumor consistency score was defined as score 0. If >1 CUSA setting was used for tumor removal, the mean value of the intraoperative tumor consistency scores was applied.

### PCT Technique

The PCT examination was performed using a 320-section multi-detector row CT scanner (Aquilion ONE; Toshiba). For the perfusion scan, 70 mL of nonionic iodinated contrast medium, iopamidol (370 mg I/mL, Imeron; Eisai) was injected at a rate of 5 mL/s through the right antecubital vein. A total of 20 volumes covering the whole brain was acquired; each volume comprised 320 images of 0.5 mm-thick sections that covered a total of 16 cm of the head in the superior-inferior direction. The first volume was acquired with an acquisition delay of 5 seconds after the injection of contrast media, allowing the acquisition of baseline images without contrast enhancement, which were used as a mask for obtaining bone subtraction. Next, 10 volumes of the brain were acquired starting at 12 seconds after the injection of contrast media at a sampling interval of 1 volume every 1 second. Then, 5 volumes were acquired starting at 22 seconds after the

injection at a sampling interval of 1 volume every 2 seconds. Subsequently, 3 volumes were acquired starting at 35 seconds after the injection at a sampling interval of 1 volume every 3 seconds. Finally, 1 volume was acquired at 47 seconds.

Block circulant singular value decomposition perfusion maps, including tumor blood flow (BF), blood volume (BV), and MTT, were calculated directly from the residue function using the PMA software. Nonparenchymal vascular voxels were automatically excluded by temporal intensity thresholding. Arterial voxels were identified automatically by identifying the vascular voxels with the earliest peak enhancement. The arterial and venous reference voxels were selected automatically under supervision. All perfusion maps were converted to 2-mm section thickness using nearest-neighbor interpolation.

### **MRE Technique**

MRE data acquisition was conducted with a spin-echo EPI MRE sequence<sup>5,6,10,11,29,30</sup> on a 3T MR imaging scanner (Discovery 750; GE Healthcare). Shear waves were introduced into the brain with a soft pillowlike passive driver designed for brain MRE that was placed under the subject's head within a 32-channel phased array coil. A pneumatic actuator (Resoundant)<sup>31</sup> that was placed outside the MR imaging examination room produced pneumatic pressure waves and vibrated the brain at a mechanical frequency of 60 Hz. 3D wavefield imaging was repeated to capture motion along the positive and negative x, y, and z directions through 6 phase offsets to observe wave propagation in time. The imaging parameters were as follows: axial slices, TR = 3600 ms, TE = 62 ms, no signal averaging, FOV = 24 × 24 cm<sup>2</sup>, acquisition matrix = 128 × 128, parallel imaging acceleration factor = 3, section thickness = 3 mm with no section gap, and acquisition time = about 5 minutes. Depending on the subject, 48–50 sections were acquired to cover the entire brain.

Stiffness maps were automatically created on the MR imaging scanner using a previously described pipeline.<sup>9</sup> In brief, stiffness maps were generated in 3 steps. In the first step, the temporal harmonic of the curl of the displacement images was calculated. In the second step, the results were smoothed with quartic smoothing kernels of the form  $(1-x^2)^2 \times (1-y^2)^2 \times (1-z^2)^2$ , where x, y, and z are linearly spaced from -1 to 1. In the third step, the first-harmonic curl wave information was calculated using a direct inversion of the Helmholtz wave equation. The complex shear modulus values were then median-filtered using a 3 × 3 × 3 median filter. Next, shear stiffness maps (elastograms), ie, the magnitude of the complex shear modulus, were created on the scanner, from which regional stiffness information could be measured.

### **Image Processing**

ROIs of the tumor were manually drawn on the magnitude images for the MRE and on the delayed postcontrast images for the PCT by a board-certified neuroradiologist with 10 years of experience, blinded to the surgical findings (T.T.). For MRE, the ROI used for reporting tumor stiffness was eroded by 3 voxels from every edge to remove edge artifacts; this procedure was previously reported as a method to minimize partial volume effects and edge-related bias.<sup>31</sup>

For perfusion metrics, we normalized the absolute quantified BF, BV, and MTT values using the brain mask created by manually contouring the brain parenchyma excluding the CSF on the delayed postcontrast images to increase the robustness of regional physiologic measures by removing variations due to the arterial input function<sup>32</sup> and variations in cardiac output.<sup>33</sup>

Maps of BF, BV, and MTT (defined as relative BF [rBF], relative BV [rBV], and relative MTT [rMTT], respectively) were calculated by dividing each voxel value by the mean value of the brain mask. The tumor volume was computed from the tumor ROI drawn on MRE magnitude images.

### **Statistical Analysis**

Correlations between stiffness and the perfusion metrics rBF, rBV, and rMTT; stiffness and the intraoperative tumor consistency score; and the perfusion metrics rBF, rBV, and rMTT and the intraoperative tumor consistency score were evaluated using the Spearman rank correlation test.

On the basis of the results of correlation analyses, patients in cohort 1 were also grouped according to the median value of stiffness in our cohort into the “high-stiffness” group ( $\geq 2.9$  kPa) or the “low-stiffness” group ( $< 2.9$  kPa). The receiver operating characteristic curve was used to investigate the predictive ability of perfusion metrics for tumor stiffness. Cutoff values of perfusion metrics were determined by maximizing the Youden index on the estimated curves. Tumor stiffness and perfusion metrics among the histologic subtypes were analyzed using a nonparametric analysis of variance (Kruskal-Wallis test) and the Steel-Dwass test for post hoc comparisons.  $P < .05$  was considered statistically significant (2-tailed). All statistical analyses were performed using commercial software (JMP, Version 13.0.0; SAS Institute).

## **RESULTS**

Patient demographics, tumor location, tumor volume, intraoperative tumor consistency score, histologic subtype, and cohort are summarized in the Online Supplemental Data. In 7 of 18 meningiomas in cohort 2, two different CUSA settings were used; therefore, the mean intraoperative tumor consistency score was applied. The mean age of the 18 patients (14 women) was 62.8 (SD, 15.3) years, and the median intraoperative tumor consistency score was 3 (range, 1–8). All cases required the use of CUSA for tumor removal. MRE measured the mean stiffness as 3.12 (SD, 1.23) kPa, and the median mean stiffness was 2.89 kPa for 18 meningiomas. The mean values of rBF, rBV, and rMTT for cohort 1 were 3.37 (SD, 2.56), 3.95 (SD, 3.19), and 1.13 (SD, 0.17), respectively.

Correlations between perfusion metrics and stiffness are shown in Fig 1. rMTT was inversely correlated with stiffness ( $r = -0.69$ ,  $P = .006$ ) (Fig 1C). However, rBF and rBV were not significantly correlated with tumor stiffness (Fig 1A, -B).

A plot of mean tumor stiffness versus the intraoperative tumor consistency score is shown in Fig 2. Stiffness was significantly positively correlated with intraoperative tumor consistency ( $r = 0.59$ ,  $P = .01$ ) (Fig 2). There was no correlation between all perfusion metrics (rBF, rBV, and rMTT) and the intraoperative tumor consistency score.

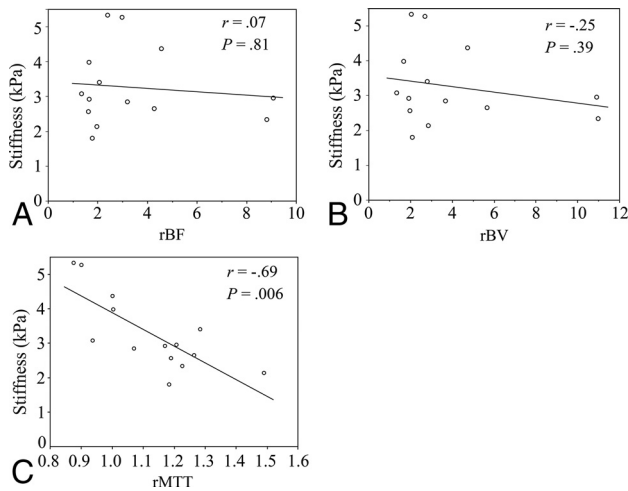


**FIG 1.** Scatterplot along with the least squares fitted line of tumor stiffness (kilopascal) measured using MRE and perfusion metrics measured using PCT in 14 patients with meningiomas. Graphs show stiffness versus rBF (A), rBV (B), and rMTT (C).

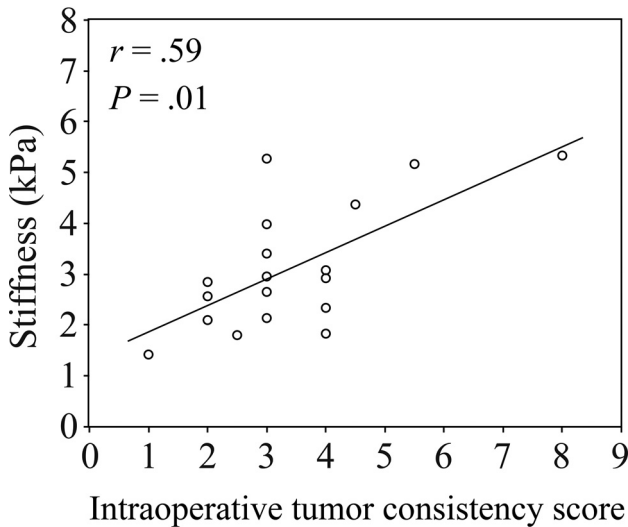


**FIG 2.** Scatterplot along with the least squares fitted line of tumor stiffness (kilopascal) measured using MRE and the intraoperative tumor consistency score in 18 patients with meningiomas.

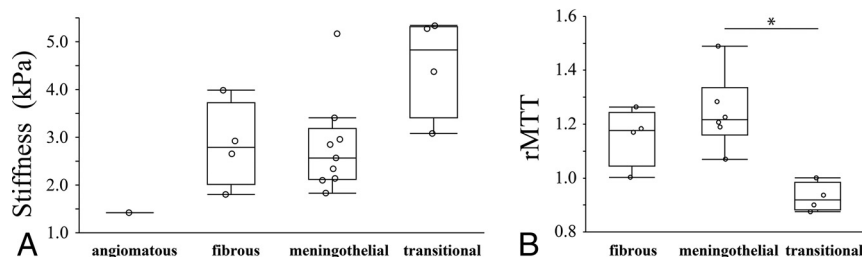


**FIG 3.** Boxplot of stiffness (kilopascal) (A) and rMTT (B) among histologic subtypes of meningioma. The lower and upper hinges of the boxes represent the 25th and 75th percentiles, respectively. The line within the box denotes the 50th percentile (median), and the whiskers indicate the maximum and minimum values. The asterisk indicates  $P < .05$  for post hoc comparisons (Steel-Dwass test).

Receiver operating characteristic analysis revealed that rMTT was a good predictor of tumors in the high-stiffness group (stiffness  $\geq 2.9$  kPa) (area under the receiver operating characteristic curve = 0.81,  $P = .02$ ). By means of a cutoff value of  $< 1.00$ , the sensitivity and specificity of rMTT for predicting tumors with high stiffness were 62.5% (5/8) and 100% (6/6), respectively.

Of the 18 meningiomas in cohort 2, nine meningothelial meningiomas, 4 fibrous meningiomas, 4 transitional meningiomas, and 1 angiomatous meningioma were pathologically confirmed, while 6 meningothelial meningiomas, 4 fibrous meningiomas, and 4 transitional meningiomas were pathologically confirmed for 14 meningiomas in cohort 1. Results from the Kruskal-Wallis test revealed significant differences in stiffness ( $P = .04$ ) (Fig 3A) and rMTT ( $P = .01$ ) (Fig 3B) among meningioma subtypes. However, there were no significant differences in rBF and rBV among meningioma subtypes. The intraoperative tumor consistency score also showed no significant differences with respect to meningioma subtypes for both cohort 1 and cohort 2. Post hoc analysis revealed that the rMTT of the transitional meningiomas was significantly lower than that of the meningothelial meningiomas ( $P = .04$ ) (Fig 3B).

Three representative meningioma cases are shown in the Online Supplemental Data. The stiffness maps (second row) and rMTT maps (bottom row) demonstrate a trend whereby rMTT decreased as stiffness increased. The rBF and rBV of a 42-year-old woman with a transitional meningioma, with a stiffness of 5.34 kPa (right column), were lower than those of a 72-year-old woman with a fibrous meningioma and stiffness of 2.65 kPa (left column). However, the rBF and rBV of the transitional meningioma of the 42-year-old woman (right column) were higher than those of a fibrous meningioma of a 62-year-old man (middle column), indicating that rBF and rBV were not necessarily correlated with the stiffness value.

## DISCUSSION

In this study, we demonstrated that rMTT measured by PCT was negatively correlated with tumor stiffness, but rBF and rBV were not. We also found that the meningioma stiffness and the intraoperative tumor consistency score were positively correlated.

An increased pathologic grading of fibrosis has been demonstrated to cause an increase in intraoperative tumor consistency in meningiomas.<sup>34</sup> Conversely, perfusion conditions, including BF or BV, are also important factors that influence stiffness. For example, increased viscoelastic parameters are correlated with increased BF in the brain<sup>21,22</sup> and increased BV in the liver.<sup>23</sup> In addition, perfusion metrics, including BV<sup>35</sup> or BF,<sup>36</sup> are positively correlated with microvascular density in meningiomas. Collectively, perfusion metrics including BF and BV and fibrosis may both intrinsically increase meningioma stiffness. Results from a previous animal experiment that used sonographic elastography indicated that vessel density and

stiffness were negatively correlated in a stiff tumor model with increasing amounts of collagen; however, vessel density and stiffness were positively correlated in a soft-tumor model with perfused cores and less collagen.<sup>25</sup> These results suggest that the degree of contribution of vascular density or fibrosis to tumor stiffness may vary according to the balance of pathologic contents. The complex relationship between vascular and fibrosis content may explain the lack of a positive correlation between BF and BV and stiffness in this study.

A marked correlation between rMTT and stiffness was observed in this study. Despite the widespread application in stroke imaging, the concept of MTT has not been as fully studied as BV in the context of oncologic imaging. MTT can be defined as the average time taken for blood to transfer between arterial inflow and venous outflow; therefore, increased MTT indicates a slow flow rate and a delayed exit of contrast agent into the venous system among tumors. MTT depends on the pathway taken by the blood traveling from arteries to veins, which depends on local tissue hemodynamics due to vascular network patterns. One possible explanation for the significant negative correlation between stiffness and rMTT in our study is that the difference in contrast agent excretion conditions due to the complexity of the intratumoral vascular pathway derived from architectural distortions caused by fibrosis within the tumor may be related to stiffness changes.

It is useful for neurosurgeons to know the stiffness of a meningioma before the operation because strategies and equipment are not the same for patients with stiff and soft tumors. Consistent with our results, previous studies have reported that MRE-measured meningioma stiffness is positively correlated with the tumor consistency assessed by a similar 5-point scale determined by surgeons.<sup>14-16</sup> In our criteria, we applied the mean value of the CUSA setting for tumors with 2 distinct consistency components (7 cases) whose value was considered to be derived from both components of the tumor. However, because the tumor margins were removed to create the final ROI, peripheral regions, such as the site of attachment of the meningioma to the dura, were not included in the stiffness measurements. Thus, the reported stiffness was likely biased toward the central areas. Therefore, the reported stiffness of internally heterogeneous tumors may have been underestimated or overestimated when the stiffer components were peripherally or centrally biased, respectively. The CUSA setting is probably not always a proper indicator of the tumor consistency. Nevertheless, our grading system highlights the possibility of estimating the CUSA settings required for tumor removal, which may be useful for the preoperative planning of meningiomas.

In this study, rMTT showed no significant correlation with intraoperative tumor consistency. A plausible explanation for the discrepancy in diagnostic ability between stiffness and rMTT might be the potentially superior diagnostic ability of MRE for intraoperative tumor consistency, in addition to reproducibility differences among the techniques. The within-subject coefficient of variation for brain shear stiffness of normal brain tissue was reportedly 1.8%–3.5% at the same mechanical frequency (60 Hz) as in our study,<sup>37</sup> however, MTT measured by PCT for normal brain tissue was reported as 8.8%.<sup>38</sup> Therefore, the potentially

higher variability expected in the reported rMTT value might lead to a lower correlation with intraoperative tumor consistency, especially with our small sample size and our scoring system, which was highly subdivided into the 11-point scale. This scoring system may have been sensitive to intraoperator variability in CUSA setting determination.

Although stiffness was highly correlated with rMTT, stiffness of the transitional meningioma and meningothelial meningioma was not significantly different, contrary to rMTT. One possible explanation for this discrepancy might be related to our postprocessing method for MRE. Because we eroded the tumor margins to create the final ROI for MRE, the reported stiffness would be biased toward the central tumor area and might not be adequately reflecting the mechanical properties of the whole tumor. In the case with considerably higher stiffness (5.17 kPa) than other cases of meningothelial meningiomas (Fig 3A), the 18th case in the Online Supplemental Data, the CUSA setting at the central area was 90%, while it was 20% in the periphery. This finding suggests that the reported stiffness was overestimated relative to the entire tumor. Another factor might be the limited statistical power due to the small sample size included in each histologic subtype and the relatively large number of subgroups. However, Sakai et al<sup>16</sup> suggested that MRE may be able to distinguish relatively firm meningiomas, such as fibrous and transitional meningiomas, from relatively soft meningiomas, such as meningothelial meningiomas; however, statistical analyses were not performed in that study. Moreover, although there was only 1 case, the stiffness of an angiomatous meningioma, typically a soft tumor,<sup>39</sup> was the lowest in all cases in our study (Fig 3A). These findings may suggest the potential relationship between stiffness and histologic subtype in meningioma. Further research with a larger sample size and a more devised postprocessing method reducing edge-related artifacts<sup>31</sup> is required to elucidate whether MRE has a potential ability to predict pathologic meningioma subtypes.

To characterize the relationship between perfusion metrics and subtypes, Zhang et al<sup>26</sup> used dynamic susceptibility contrast perfusion MR imaging and reported that the tumoral BV of angiomatous meningiomas was significantly higher than that of meningothelial, fibrous, or anaplastic meningiomas. Additionally, Kimura et al<sup>28</sup> used spin-labeling perfusion MR imaging and reported that the BF was significantly increased in angiomatous meningiomas compared with that in fibrous and meningothelial meningiomas. Nevertheless, these reports focused on the differentiation between angiomatous meningioma, which is typically a soft and vascular-rich tumor,<sup>39</sup> and other subtypes that are not as vascular. However, as discussed above, the relationship between fibrosis and vascular density may confound each other in a complex manner; therefore, we cannot apply their results to our comparison between consistency and perfusion metrics.

This study had several limitations. First, the number of subjects was small, particularly the number of subjects with high intraoperative tumor consistency. Therefore, the current results might be too susceptible to outlier data to be clinically meaningful. Future prospective studies with larger sample sizes and more uniformly distributed data are necessary to confirm our preliminary results. Second, although we used an intraoperative tumor

consistency score based on the CUSA setting that was applied for tumor removal in an effort to establish a quantitative method, the use of this analysis with the erosion of edge pixels from the ROIs to manage edge artifacts may have resulted in a disagreement between intraoperative assessment and imaging parameters based on the location of stiffer/softer components in internally heterogeneous tumors. Therefore, applying a method that accounts for spatial variability in the stiffness or perfusion metrics and allows a more detailed comparison based on each distinct component of the tumor is preferable. Third, our study lacked an examination of the histopathologic components corresponding to tumor stiffness and perfusion metrics. An investigation of the histopathologic determinants underpinning stiffness or perfusion metrics, including collagenous content, cellular architecture (including cellular arrangement, size, or density), and vascular density/network conditions is required in future work.

## CONCLUSIONS

This study demonstrated the relationship between stiffness and perfusion metrics, the correlation between stiffness and intraoperative tumor consistency, and the differences in perfusion metrics among common histologic subtypes of meningiomas. The results show that tumor stiffness may be useful to predict intraoperative tumor consistency, rMTT may correlate with tumor stiffness, and rMTT may be potentially useful to differentiate histologic subtypes in meningioma.

Disclosures: Kevin J. Glaser—*RELATED: Grant:* National Institutes of Health, *Comments:* R37-EB001981\*; *Comments:* The Mayo Clinic and Kevin J. Glaser have intellectual property rights and a financial interest related to magnetic resonance elastography technology. Richard L. Ehman—*RELATED: Grant:* National Institutes of Health, *Comments:* R37 EB001981\*; *Other Relationships:* The Mayo Clinic and Richard L. Ehman have intellectual property rights and a financial interest in magnetic resonance elastography technology. \*Money paid to the institution.

## REFERENCES

- Louis DN, Perry A, Reifenberger G, et al. **The 2016 World Health Organization Classification of Tumors of the Central Nervous System: a summary.** *Acta Neuropathol* 2016;131:803–20 [CrossRef Medline](#)
- Kendall B, Pullicino P. **Comparison of consistency of meningiomas and CT appearances.** *Neuroradiology* 1979;18:173–76 [CrossRef Medline](#)
- Shiroishi MS, Cen SY, Tamrazi B, et al. **Predicting meningioma consistency on preoperative neuroimaging studies.** *Neurosurg Clin N Am* 2016;27:145–54 [CrossRef Medline](#)
- Muthupillai R, Lomas DJ, Rossman PJ, et al. **Magnetic resonance elastography by direct visualization of propagating acoustic strain waves.** *Science* 1995;269:1854–57 [CrossRef Medline](#)
- Arani A, Murphy MC, Glaser KJ, et al. **Measuring the effects of aging and sex on regional brain stiffness with MR elastography in healthy older adults.** *Neuroimage* 2015;111:59–64 [CrossRef Medline](#)
- ElSheikh M, Arani A, Perry A, et al. **MR elastography demonstrates unique regional brain stiffness patterns in dementias.** *AJR Am J Roentgenol* 2017;209:403–08 [CrossRef Medline](#)
- Hiscox LV, Johnson CL, McGarry MD, et al. **High-resolution magnetic resonance elastography reveals differences in subcortical gray matter viscoelasticity between young and healthy older adults.** *Neurobiol Aging* 2018;65:158–67 [CrossRef Medline](#)
- Sack I, Streitberger KJ, Krefling D, et al. **The influence of physiological aging and atrophy on brain viscoelastic properties in humans.** *PLoS One* 2011;6:e23451 [CrossRef Medline](#)
- Takamura T, Motosugi U, Sasaki Y, et al. **Influence of age on global and regional brain stiffness in young and middle-aged adults.** *J Magn Reson Imaging* 2020;51:727–33 [CrossRef Medline](#)
- Murphy MC, Huston J 3rd, Jack CR Jr, et al. **Decreased brain stiffness in Alzheimer's disease determined by magnetic resonance elastography.** *J Magn Reson Imaging* 2011;34:494–98 [CrossRef Medline](#)
- Murphy MC, Jones DT, Jack CR Jr, et al. **Regional brain stiffness changes across the Alzheimer's disease spectrum.** *Neuroimage Clin* 2016;10:283–90 [CrossRef Medline](#)
- Lipp A, Trbojevic R, Paul F, et al. **Cerebral magnetic resonance elastography in supranuclear palsy and idiopathic Parkinson's disease.** *Neuroimage Clin* 2013;3:381–87 [CrossRef Medline](#)
- Bunecivicius A, Schregel K, Sinkus R, et al. **REVIEW: MR elastography of brain tumors.** *Neuroimage Clin* 2020;25:102109 [CrossRef Medline](#)
- Hughes JD, Fattahi N, Van Gompel J, et al. **Higher-resolution magnetic resonance elastography in meningiomas to determine intra-tumoral consistency.** *Neurosurgery* 2015;77:653–58; discussion 658–59 [CrossRef Medline](#)
- Murphy MC, Huston J 3rd, Glaser KJ, et al. **Preoperative assessment of meningioma stiffness using magnetic resonance elastography.** *J Neurosurg* 2013;118:643–48 [CrossRef Medline](#)
- Sakai N, Takehara Y, Yamashita S, et al. **Shear stiffness of 4 common intracranial tumors measured using MR elastography: comparison with intraoperative consistency grading.** *AJNR Am J Neuroradiol* 2016;37:1851–59 [CrossRef Medline](#)
- Xu L, Lin Y, Han JC, et al. **Magnetic resonance elastography of brain tumors: preliminary results.** *Acta Radiol* 2007;48:327–30 [CrossRef Medline](#)
- Yin Z, Hughes JD, Glaser KJ, et al. **Slip interface imaging based on MR-elastography preoperatively predicts meningioma-brain adhesion.** *J Magn Reson Imaging* 2017;46:1007–16 [CrossRef Medline](#)
- Parker KJ. **Experimental evaluations of the microchannel flow model.** *Phys Med Biol* 2015;60:4227–42 [CrossRef Medline](#)
- Le Bihan D. **Theoretical principles of perfusion imaging: application to magnetic resonance imaging.** *Invest Radiol* 1992;27:(Suppl 2):6–11 [CrossRef Medline](#)
- Chatelin S, Humbert-Claude M, Garteiser P, et al. **Cannabinoid receptor activation in the juvenile rat brain results in rapid biomechanical alterations: neurovascular mechanism as a putative confounding factor.** *J Cereb Blood Flow Metab* 2016;36:954–64 [CrossRef Medline](#)
- Hetzer S, Birr P, Fehlner A, et al. **Perfusion alters stiffness of deep gray matter.** *J Cereb Blood Flow Metab* 2018;38:116–25 [CrossRef Medline](#)
- Dittmann F, Tzschatzsch H, Hirsch S, et al. **Tomoelastography of the abdomen: tissue mechanical properties of the liver, spleen, kidney, and pancreas from single MR elastography scans at different hydration states.** *Magn Reson Med* 2017;78:976–83 [CrossRef Medline](#)
- Jamin Y, Boulton JK, Li J, et al. **Exploring the biomechanical properties of brain malignancies and their pathologic determinants in vivo with magnetic resonance elastography.** *Cancer Res* 2015;75:1216–24 [CrossRef Medline](#)
- Riegler J, Labyed Y, Rosenzweig S, et al. **Tumor elastography and its association with collagen and the tumor microenvironment.** *Clin Cancer Res* 2018;24:4455–67 [CrossRef Medline](#)
- Zhang H, Rodiger LA, Shen T, et al. **Perfusion MR imaging for differentiation of benign and malignant meningiomas.** *Neuroradiology* 2008;50:525–30 [CrossRef Medline](#)
- Zikou A, Alexiou GA, Goussia A, et al. **The role of diffusion tensor imaging and dynamic susceptibility perfusion MRI in the evaluation of meningioma grade and subtype.** *Clin Neurol Neurosurg* 2016;146:109–15 [CrossRef Medline](#)
- Kimura H, Takeuchi H, Koshimoto Y, et al. **Perfusion imaging of meningioma by using continuous arterial spin-labeling: comparison with dynamic susceptibility-weighted contrast-enhanced MR images and histopathologic features.** *AJNR Am J Neuroradiol* 2006;27:85–93 [Medline](#)

29. Fattahi N, Arani A, Perry A, et al. **MR elastography demonstrates increased brain stiffness in normal pressure hydrocephalus.** *AJNR Am J Neuroradiol* 2016;37:462–67 [CrossRef Medline](#)
30. Huston J 3rd, Murphy MC, Boeve BF, et al. **Magnetic resonance elastography of frontotemporal dementia.** *J Magn Reson Imaging* 2016;43:474–78 [CrossRef Medline](#)
31. Murphy MC, Huston J 3rd, Jack CR Jr, et al. **Measuring the characteristic topography of brain stiffness with magnetic resonance elastography.** *PLoS One* 2013;8:e81668 [CrossRef Medline](#)
32. Kamath A, Smith WS, Powers WJ, et al. **Perfusion CT compared to H(2) (15)O/O (15)O PET in patients with chronic cervical carotid artery occlusion.** *Neuroradiology* 2008;50:745–51 [CrossRef Medline](#)
33. Klotz E, König M. **Perfusion measurements of the brain: using dynamic CT for the quantitative assessment of cerebral ischemia in acute stroke.** *Eur J Radiol* 1999;30:170–84 [CrossRef Medline](#)
34. Phuttharak W, Boonrod A, Thammaroj J, et al. **Preoperative MRI evaluation of meningioma consistency: a focus on detailed architectures.** *Clin Neurol Neurosurg* 2018;169:178–84 [CrossRef Medline](#)
35. Shi R, Jiang T, Si L, et al. **Correlations of magnetic resonance, perfusion-weighted imaging parameters and microvessel density in meningioma.** *J BUON* 2016;21:709–713 [Medline](#)
36. Koizumi S, Sakai N, Kawaji H, et al. **Pseudo-continuous arterial spin labeling reflects vascular density and differentiates angiomatous meningiomas from non-angiomatous meningiomas.** *J Neurooncol* 2015;121:549–56 [CrossRef Medline](#)
37. Huang X, Chafi H, Matthews KL 2nd, et al. **Magnetic resonance elastography of the brain: a study of feasibility and reproducibility using an ergonomic pillow-like passive driver.** *Magn Reson Imaging* 2019;59:68–76 [CrossRef Medline](#)
38. Lee TY, Nabavi DG, Lee DH, et al. **Quantitative CT perfusion measurement: normal values and reproducibility in man.** *Stroke* 2000;32:344–45 [https://www.ahajournals.org/doi/10.1161/str.32.suppl\\_1.344-e](https://www.ahajournals.org/doi/10.1161/str.32.suppl_1.344-e). Accessed April 15, 2020
39. Maiuri F, Iaconetta G, de Divitiis O, et al. **Intracranial meningiomas: correlations between MR imaging and histology.** *Eur J Radiol* 1999;31:69–75 [CrossRef Medline](#)